Plasmonic microcavity formed by the Möbius strip*

Yang Zeng(曾扬)†, Zhi-Yong Wang(王智勇), Yuan Wu(吴远), Lan-Song Lu(陆兰松), Yun-Xiang Wang(王云祥), Shuang-Jin Shi(史双瑾), and Qi Qiu(邱琪)

School of Optoelectronic Information, University of Electronic Science and Technology of China, Chengdu 610054, *China*

(Received 17 August 2016; revised manuscript received 3 December 2016; published online 13 February 2017)

We propose a Möbius-strip-type plasmonic cavity with a silver Möbius strip sandwiched between dielectric layers. By brief theoretical and simulation analyses, we obtain that the Q factor of the cavity remains about 40 and the mode volume is ultrasmall (less than 1 μm^3) which is more compact than that of the cylindric cavity. This Möbius-strip-type plasmonic cavity supporting the propagation of surface plasmon polaritons owns some unusual properties such as more effective volume and the spatial separation. More potential applications based on this cavity remain to be explored in future nanophotonics.

Keywords: suface plamons, optical resonator

PACS: 73.20.Mf, 42.60.Da **DOI:** 10.1088/1674-1056/26/3/037303

1. Introduction

Optical microcavities confine light into small volumes by resonant recirculation.[1] The devices on the basis of optical microcavities attract numerous studies and have realized a wide range of applications, such as strong-coupling cavity quantum electrodynamics (QED),[2,3] enhancement and suppression of spontaneous emission,[4] novel sources,[5] and dynamic filters in optical communication.[1] In recent years, biological and chemical sensors have also been highly developed, which mainly benefits from optical microcavities.[6,7] However, conventional optical microcavities have the limitation to size reduction due to the existence of the diffraction limit, which becomes a chief obstacle to miniaturize optical devices.

Recently, it was reported that the plasmonic microcavities[8–10] have overcome these difficulties. Plasmonic microcavities are based on the effect of surface plasmon polaritons (SPPs) that is capable of confining an electromagnetic field on the surface on a subwavelength scale and therefore provides the possibility of breaking the diffraction limit significantly, which shows great promise in miniaturizing photonic integrated circuits.[11,12] As a consequence, ultrasmall mode volume is accessible; nevertheless, plasmonic device suffers a low Q factor (generally less than 100) primarily due to the existence of radiation loss and Ohmic loss in metal at room temperature. The employment of rotational symmetry structure[13–16] could help to lessen the loss above to some extent. The exploration of new structural design is still in progress for the sake of better properties of cavities in different application areas.

The Möbius strip is a curious structure and its basic geometric configuration is a surface with only one side and only one boundary,[17] as shown in Fig. 1(a). Vividly and popularly speaking, if an ant were to crawl along the length of this strip, it would return to its starting point after having traversed the entire length of the strip (on both sides of the original strip) without ever crossing an edge. The Möbius strip has the mathematical property of being non-orientable and can be realized as a ruled surface. Some creative applications based on this unique structure present the original frontier of technology, such as an inductionless resistor,[18] superconductors with high transition temperature,[19] and graphene volume.[20]

In this paper, we will propose a novel Möbius-strip-type plasmonic cavity with dimension of several microns (specifically a silver Möbius strip sandwiched between dielectric layers as shown in Fig. 1(b)) and study its peculiar properties theoretically. We take an appropriate size of the cavity such that one of its resonant wavelengths approaches the telecom wavelength (1550 nm) for practicality.

2. Theoretical model

As is well known, the primary parameters of plasmonic microcavities consist of a Q factor, mode volume and the Purcell factor. The Q factor relates to the dissipation rate of photons confined into the cavity. More practically, the calculated Q factors are comprised of contributions from intrinsic metal loss and the geometry- and material-dependent radiation loss into free space, i.e., $Q^{-1} \approx Q_{\text{metal}}^{-1} + Q_{\text{rad}}^{-1}$. The typical Q factor of the plasmonic microcavity is less than 100, while the outstanding work from Min *et al.* experimentally demonstrated a high-Q plasmonic whispering gallery microdisk fabricated by coating the surface of a high-Q silica micro-resonator with a thin layer of silver.[13] Albeit the Q factor exceeds 1000 in the

*Projected supported by the National Natural Science Foundation of China (Grant Nos. 61271030 and 61308041) and the Fundamental Research Funds for the Central Universities of China (Grant No. ZYGX2014J043).

†Corresponding author. E-mail: 201422050125@std.uestc.edu.cn

© 2017 Chinese Physical Society and IOP Publishing Ltd

near infrared region, which is close to the theoretical metal-loss-limited Q factor, the mode volume remains still high.

The mode volume measures the spatial extent of the modal field inside the cavity, defined as the ratio of the total energy density of the mode to the peak energy density, i.e., $V_{\text{eff}} = \int \varepsilon \boldsymbol{E}^2 \mathrm{d}^3 r / \max(\varepsilon \boldsymbol{E}^2)$. The mode volume of a classic reported ring-type plasmonic micro-resonator is capable of being achieved to be less than 1 μm^3 [21,22] with a relatively high Q factor.

The Purcell factor refers to the emission rate enhancement of a spontaneous emitter inside a cavity or resonator and plays a central role in nonlinear optics and light–matter interaction. Its expression formula is expressed as

$$F_{\text{p}} = \frac{3}{4\pi^2}\left(\frac{\lambda_0}{n}\right)^3 \left(\frac{Q}{V_{\text{eff}}}\right), \tag{1}$$

where λ_0 is the resonant wavelength and n is the refractive index of the gain medium. The Purcell factor is frequently employed as a tradeoff between Q factor and mode volume.

We will design a plasmonic microcavity formed by a Möbius strip and study its properties theoretically. Because of the surface along the length of the Möbius strip without boundary, the surface wave becomes a standing wave. Obviously, the distance from one side to the opposite side along the length of the strip clockwise equals the one in the anticlockwise case. As a consequence, there are two different modes formed on the Möbius strip: odd mode and even mode (the more visual statement is attached to the Appendix A). In addition, the boundary conditions of the Möbius strip must be introduced as follows:[23]

$$\psi(x+L_x, y) = \psi(x, -y), \qquad \text{Möbius BC}, \tag{2}$$

$$\psi(x, -L_y/2) = \psi(x, L_y/2) = 0, \qquad \text{Dirichlet BC}, \tag{3}$$

where $\psi(x,y)$ represents the electromagnetic field density, L_x and L_y refer to the circumference and the width of the Möbius strip respectively (the corresponding coordinate is shown in blue in Fig. 1(a), which is along the surface). Equation (2) implies that the signs of opposite wave fields along the y-axis must be reversed; namely, here wave crests/troughs front crests/troughs in the odd mode and wave crests/troughs front another on the opposite surface in the even mode. Equation (3) simply restricts the condition that any wave field must attenuate to 0 at the edge. Moreover, SPPs are strongly bound to the interface and evanescently decay in the direction perpendicular to the surface of the Möbius strip. According to all mentioned above, we obtain the general impression of SPPs modes on the Möbius strip.

In our simulation experiment, the main component of the proposed Möbius-strip-type plasmonic cavity is a silver Möbius strip shown in Fig. 1(a), sandwiched between dielectric layers (actually the opposite layers belong to one) and the entire plasmonic cavity is shown in Fig. 1(b). With the purpose of practical application near telecom wavelength (1550 nm), the values of radius R and width h of the silver strip are taken to be 0.8 μm and 0.4 μm respectively. On account of field decay in metal, the thickness of silver t is recommended to be large enough, which is fixed to 0.2 μm here to avoid the interference from the opposite side directly through the metal. The thickness of the dielectric layer d is set to be 0.2 μm for the exhibition of a pure surface plasmonic mode appropriately without any other hybrid modes.

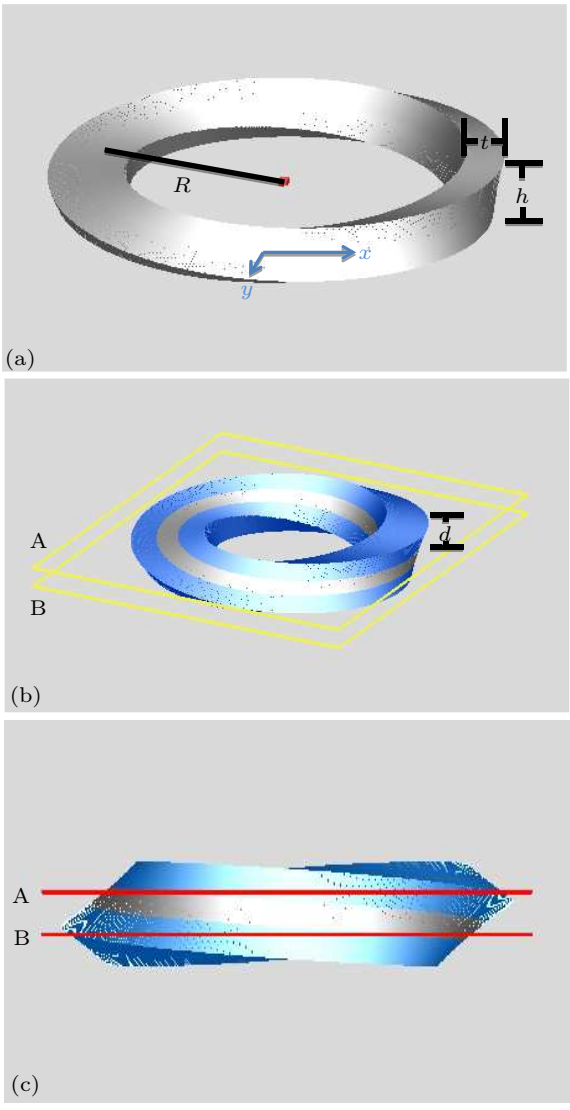


Fig. 1. (color online) (a) Sketching of the silver Möbius strip. Here the material is silver. $R = 0.8$ μm, $h = 0.4$ μm and $t = 0.2$ μm. (b) Schematic of the Möbius-strip-type plasmonic cavity. The geometry is a silver Möbius strip sandwiched between dielectric layers. The thickness of dielectric layer $d = 0.2$ μm. "A" and "B" refer to the cross sections at 20 nm above the silver strip and 20 nm below respectively. (c) Right view of the cavity presents another perspective of the relative position of sections "A" and "B".

3. Simulation analysis

Our simulation analysis is performed by using the commercial software Lumerical FDTD Solutions[24] via the FDTD (finite-difference time-domain) method. The permittivity of

the silver used in the simulations comes from the experimental data by Palik[25] and here we select InP as the material of dielectric layers. In Fig. 2, the normalized peak magnitudes of H (magnetic field vector) are plotted versus wavelength ranging from 1.3 to 2.3 μm (the image blurs above 2.3 μm and the hybrid whispering gallery mode[26,27] emerges below 1.3 μm) and each wave crest represents a mode of SPPs, listed in detail in Table 1.

Figure 3 shows the profiles of electromagnetic field distribution of the proposed Möbius-strip-type plasmonic cavity. The left column expresses the odd mode with mode number

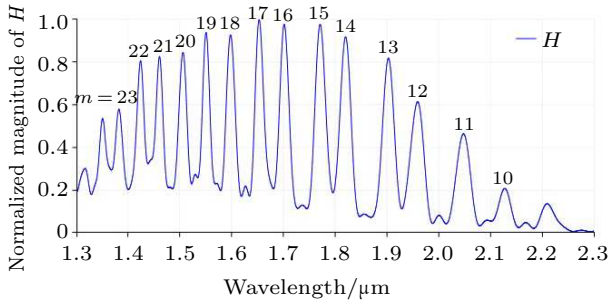


Fig. 2. (color online) Normalized peak magnitude of H (at a given location on the Möbius strip) versus wavelength ranging from 1.3 to 2.3 μm. Each wave crest represents a mode of SPPs and their specific mode numbers are labeled correspondingly.

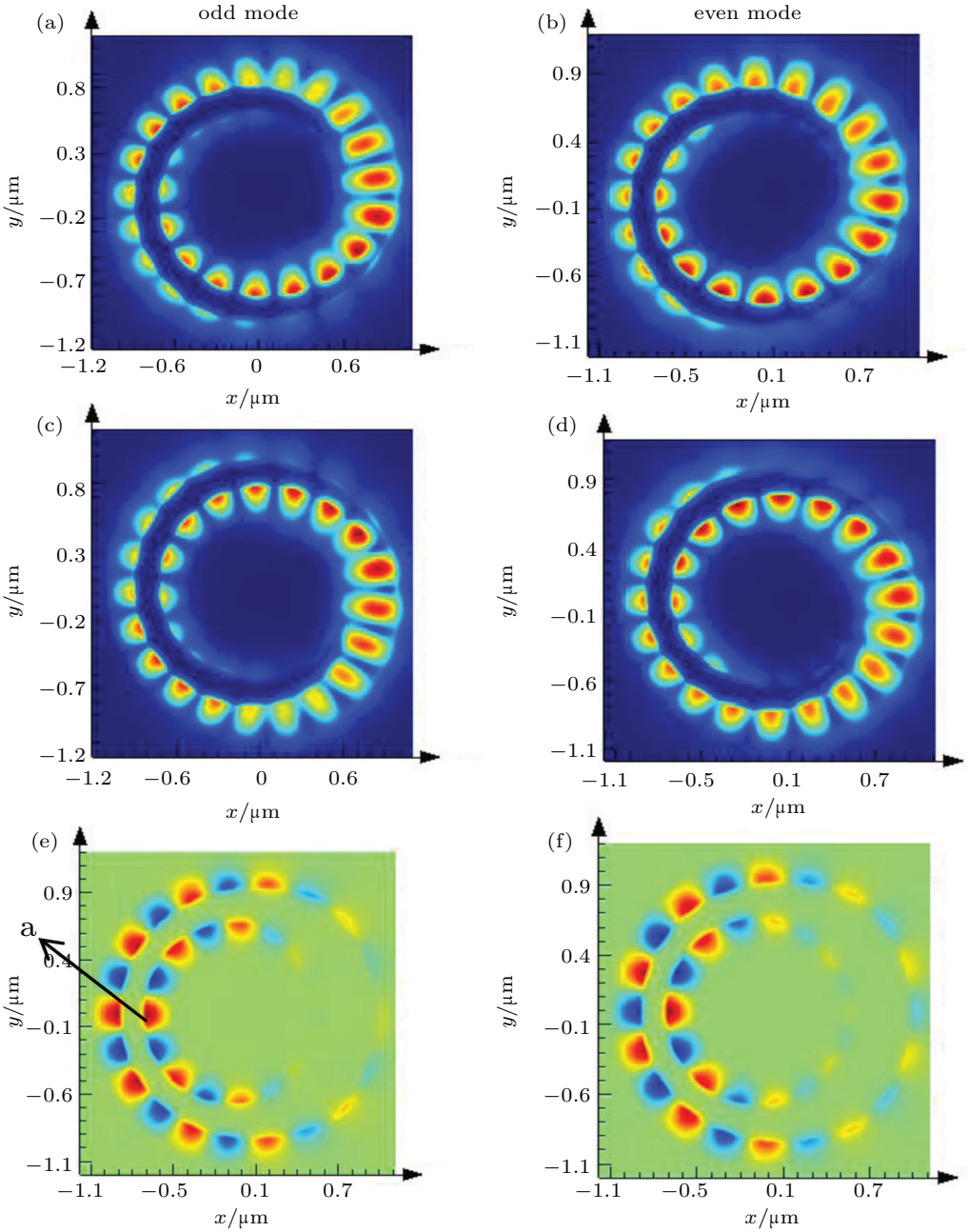


Fig. 3. (color online) Profiles of electromagnetic field distribution, showing the odd mode with mode number $m = 19$ at a wavelength of 1550 nm (on the left column) and the even mode with mode number $m = 18$ at a wavelength of 1597 nm (on the right column). Panels (a) and (b) show cross sections of magnetic field distribution H at 20 nm above, panels (c) and (d) display cross sections of magnetic field distribution H at 20 nm below and panels (e) and (f) present the profiles of magnetic field component distribution H_z in the middle.

$m = 19$ at a wavelength of 1550 nm and the right column describes the even mode with mode number $m = 18$ at 1597 nm. Figures 3(a) and 3(b) demonstrate the cross sections of magnetic field distribution H at 20 nm above the Möbius strip (depicted as cross section "A" in Figs. 1(b) and 1(c)), while figures 3(c) and 3(d) show the images 20 nm below (depicted as cross section "B" in Figs. 1(b) and 1(c)). We can conclude that the profiles of magnetic field distribution exhibit the features of SPPs, specifically the evanescently decaying perpendicularly away from the surface and zero field intensity at edges. Moreover, the mode number can be figured out from the profiles above. Figures 3(e) and 3(f) describe the profiles of representative magnetic field component distribution H_z (here the Cartesian coordinate is adopted) in the odd mode and even mode respectively, so as to further elucidate the mode confinement, and we can find the theoretical relationship between wave crest and trough, which has been analyzed before at location "a" labeled in Fig. 3(e). That is, for magnetic field component distribution H_z, the wave crests/troughs front crests/troughs in the odd mode (see Fig. 3(e)) and wave crests/troughs front wave troughs/crests in the even mode (see Fig. 3(f)). Up to now, we have presented the description of SPP modes on the Möbius strip.

What we are concerned most is the performances of the plasmonic cavity: Q factor, mode volume, and the Purcell factor. Table 1 indicates the above-mentioned parameters in detail. As can be seen from the column of Q factor, the fluctuation of Q factors is mild and numerical values are larger than 40. Our data also reveal that different modes or resonant wavelengths have little influence on the Q factor. As a consequence, some other effective methods may help improve the Q factor, such as the employment of gain materials[28] and the enlargement of cavity dimension.[21]

Table 1. Performances of the Möbius-strip-type cavity with different modes.

Odd mode					Even mode				
λ/nm	m	Q	$V/\mu m^3$	F_p	λ/nm	m	Q	$V/\mu m^3$	F_p
1381	23	43.2	0.39	0.86	1423	22	40.2	0.40	0.87
1460	21	42.7	0.42	1.01	1505	20	42.1	0.44	1.01
1550	19	43.3	0.44	1.21	1597	18	47.8	0.46	1.13
1652	17	38.9	0.47	1.52	1701	16	47.9	0.48	1.56
1770	15	47.8	0.51	1.91	1819	14	47.2	0.54	2.16
1902	13	48.6	0.55	1.83	1959	12	48.1	0.56	3.03
2047	11	49.3	0.62	1.62	2127	10	45.5	0.67	4.21

Another conclusion is that the mode volume increases linearly as wavelength enlarges but still maintains an ultrasmall volume as expected, which is less than 1 μm^3, and this superiority of plasmonic cavity is inherited by our Möbius-strip-type cavity. The approximate trend that the Purcell factor is raised unsteadily is predominantly attributed to the enlargement of the wavelength and the negative effect of mode volume, as Eq. (1) suggests. The Purcell factor of the even mode increases monotonically with increasing wavelength, while it is not applicable for the odd mode, which is another remarkable difference between the two modes.

To gain a better insight into the performance of the Möbius-strip-type cavity, we make a comparison with a cylindric cavity with approximately the same dimension. The schematic diagram of the cylindric cavity is shown in Fig. 4(a) (a silver ring sandwiched between dielectric layers) and the profile of electromagnetic field distribution is exhibited in Fig. 4(b). SPPs are default on the inner circumference, so there is no distinction between the odd and even modes of the cylindric cavity in contrast to the Möbius-strip-type cavity.

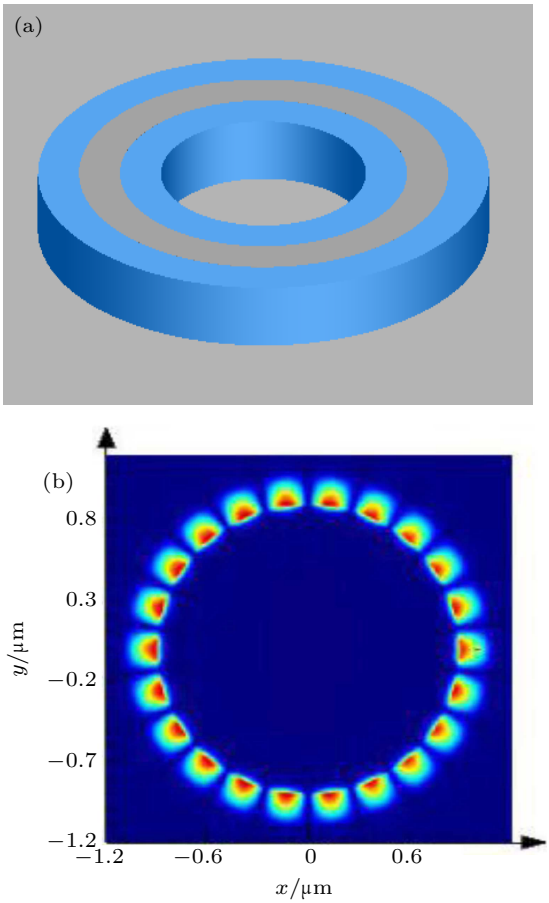


Fig. 4. (color online) (a) Schematic diagram of the cylindric cavity. The main dimension is the same as those of the Möbius-strip-type cavity for a strict comparison. (b) The cross section profile of magnetic field distribution in the middle. The example shows the mode $m = 11$ at a wavelength of 1533 nm.

Table 2 presents the same primary parameters at resonant wavelengths ranging from 1.2 to 2.3 μm. The Q factors, which are around 50, slightly exceed that of the Möbius-strip-type cavity due to a more symmetric structure. Compared with the cylindric cavity, the Möbius-strip-type cavity supports double circumference with the same radius. As a consequence, this superiority makes the effective volume of the Möbius-strip-type cavity larger than that of the cylindric cavity and provides more spaces for the light–matter interactions.

Table 2. Performances of the cylindric cavity with different resonant wavelengths.

Wavelength/nm	Mode number	Q	$V/\mu m^3$	F_p
1220	16	65.9	0.198	0.66
1266	15	64.5	0.213	0.74
1329	14	48.0	0.217	0.85
1386	13	54.7	0.230	0.93
1458	12	52.5	0.239	1.13
1533	11	53.6	0.252	1.38
1617	10	51.1	0.264	1.74
1713	9	48.3	0.276	2.07
1820	8	45.0	0.285	2.61
1931	7	42.8	0.302	3.27
2064	6	42.5	0.365	3.77
2224	5	46.0	0.379	4.06

Moreover, the appropriate comparison of mode volume should be developed between the m mode in the cylindric cavity and the $2 \times m$ mode in the Möbius-strip-type cavity (that is doubling the cylindric cavity to fulfill the perimeter equality of two cavities, here $m = 5$–11), and the latter mode volumes are supposed to be twice as large as the formers' at the same mode number correspondingly. Table 3 shows the contrast between two kinds of cavities under the revised stipulation and it concludes that the mode volumes of the Möbius-strip-type cavity are all slightly less than the expected values discussed above. This result implies that the mode volume of the Möbius-strip-type cavity is more compact than that of the cylindric cavity, which is an important merit of the Möbius-strip-type cavity.

Table 3. Revised contrast between two kinds of cavities of mode volumes.

m	V of Möbius-strip/μm^3	Revised V of cylinder/μm^3
22	0.40	0.50
20	0.44	0.53
18	0.46	0.55
16	0.48	0.57
14	0.54	0.60
12	0.56	0.73
10	0.67	0.76

Another novel character is related to the single-side feature of the Möbius-strip type. In virtue of the constraint of SPPs on the metal surface, the paths of SPPs or surface waves are simply guided by the metal. In a local area, the metal layer separates dielectric or space into two sides which neither contact nor interfere with each other directly; nevertheless, by the control of one side, it is convenient to tune SPPs (which will propagate along the surface) on the opposite side (shown in Fig. 5), which is attributed to the existence of only one surface on the Möbius strip. As a result, two sides are connected via surface waves. This speciality affords a platform for the special circumstance in need of the interaction between SPPs but which are separated by an obstacle. Another noteworthy character is that the directions of the propagations of SPPs are the same on the opposite sides (as indicated by the arrows in Fig. 5) and more relevant properties are under research. Undesirably, the process of fabrication seems to be inconvenient due to the loss of rotational symmetry. The proposed Möbius-strip-type plasmonic cavity may open up possibilities for future applications in nanophotonics, such as the update of photonic integrated circuits in device engineering.

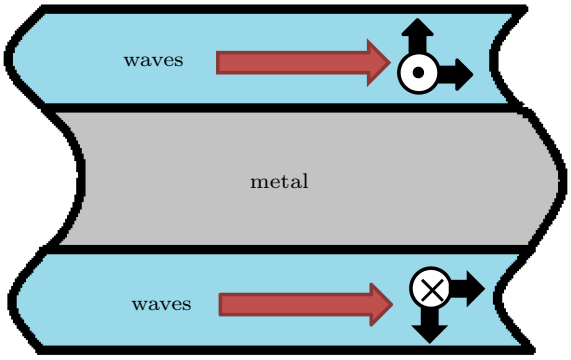


Fig. 5. (color online) Diagram of spatial separation. In this local area, the obstacle (here which is metal) separates space into two sides (colored in blue), neither of which is capable of contacting the other side directly. Attributed to the single-surface property of the Möbius strip, surface waves can reach the opposite side and indirect tuning is achievable.

4. Conclusions

We have investigated the SPPs modes in a novel Möbius-strip-type plasmonic cavity. Two modes (the odd and even mode) are distinguished by the performance of magnetic field component distribution H_z. The Q factor is more than 40 and ultrasmall mode volume is achieved, typically less than 1 μm^3, which is more compact than that of the cylindric cavity. Attributed to the novel structure, the Möbius-strip-type plasmonic cavity has some extraordinary properties such as more effective volume and the spatial separation. In summary, the Möbius-strip-type plasmonic cavity exhibits similar Q factors to those of the cylinder one and less mode volumes, which is the main merit. The Möbius-strip-type plasmonic cavity is competent to the work that the cylinder cavity does, such as spontaneous emission control and low-threshold microlasers. Its novel structure may be suited to other special applications. Other original work on the basis of SPPs on the Möbius strip and more potential applications in future nanophotonics both deserve further exploration.

Appendix A: Statement on the relationship between wave crest and trough along the surface of the Möbius strip

The stable standing waves will form on the surface of the Möbius strip as mentioned above. Here, for visual explanation, we use symbol "+" to express wave crest and "−" to represent wave trough. Figure A1(a) simply simulates the ordinary form of the odd mode (for $n = 3$) , i.e., how the wave crests and troughs arrange and we can conclude that the wave

crests propagating along the strip from one side to the opposite side will reverse into wave troughs and vice versa (as indicated by the red circles). Figure A1(b) simulates the ordinary form of the even mode (for $n = 4$). In the even mode, whatever wave crests or wave troughs, the type keeps the same as that on the other side. Figures A1(a) and A1(b) are just the sketch maps in a local area for reference only.

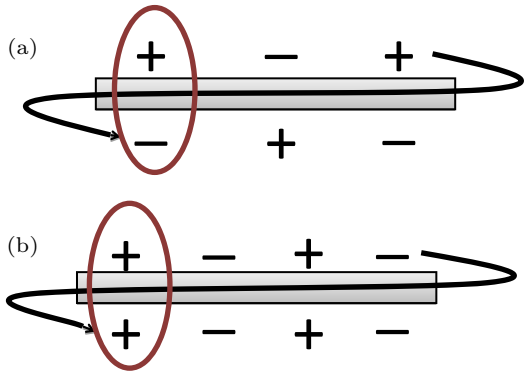


Fig. A1. (color online) Arrangement of the wave crests and troughs in (a) odd mode ($n = 3$), and (b) even mode ($n = 4$).

However, owing to the special structure of the Möbius strip equation (2) implies that the sign of the opposite wave field along the y-axis (the direction along the width of the strip) must be reversed: namely, here wave crests/troughs front crests/troughs in the odd mode and wave crests/troughs front another on the opposite surface in the even mode. In conclusion, the emulational images in Figs. 3(e) and 3(f) are consistent with the above analyses. Now, we have explained the relationship between wave vectors indicated in Figs. 3(e) and 3(f) and their physical meanings.

References

[1] Vahala K J 2003 *Nature* **424** 839
[2] Thompson R J, Rempe G and Kimble H J 1992 *Phys. Rev. Lett.* **68** 1132
[3] Mabuchi H, Turchette Q A, Chapman M S and Kimble H J 1996 *Opt. Lett.* **21** 1393
[4] Yamamoto Y, Tassone F and Cao H 2000 *Semiconductor Cavity Quantum Electrodynamics* (New York: Springer)
[5] Deppe D G, Huffaker D L, Oh T O, Deng H Y and Deng Q 1997 *IEEE J. Select. Top. Quantum Elect.* **3** 893
[6] Cooper M A 2002 *Nat. Rev. Drug Discov.* **1** 515
[7] Vollmer F and Arnold S 2008 *Nature Methods* **5** 591
[8] Ditlbacher H, Hohenau A, Wagner D, Kreibig U, Rogers M, Hofer F, Aussenegg F R and Krenn J R 2005 *Phys. Rev. Lett.* **95** 257403
[9] Bozhevolnyi S I, Volkov V S, Devaux E, Laluet J Y and Ebbesen T W 2006 *Nature* **440** 508
[10] Weeber J C, Bouhelier A, Colas des Francs G, Markey L and Dereux A 2007 *Nano Lett.* **7** 1352
[11] Barnes W L, Dereux A and Ebbesen T W 2003 *Nature* **424** 824
[12] Pacifici D, Lezec H J and Atwater H A 2007 *Nat. Photon.* **1** 402
[13] Min B, Ostby E, Sorger V, Ulin-Avila E, Yang L, Zhang X and Vahala K 2009 *Nature* **457** 455
[14] Kuttge M, García de Abajo F J and Polman A 2010 *Nano Lett.* **10** 1537
[15] Xiao Y F, Zou C J, Li B B, Li Y, Dong C H, Han Z F and Gong Q 2010 *Phys. Rev. Lett.* **105** 153902
[16] Kwon S H, Kang J H, Seassal C, Kim S K, Regreny P, Lee Y H, Lieber C M and Park H G 2010 *Nano Lett.* **10** 3679
[17] https://en.wikipedia.org/wiki/M%C3%B6bius_strip
[18] Richard D (U.S. Patent) 3 267 406 [1966-8-16]
[19] Perez-Enriquez R 2002 *Rev. Mex. Fis.* **48** (supplement 1) 262
[20] Yamashiro A, Shimoi Y, Harigaya K and Wakabayashi K 2004 *Physica E* **22** 688
[21] Xiao Y F, Li B B, Jiang X, Hu X Y, Li Y and Gong Q H 2010 *J. Phys. B* **43** 035402
[22] Zou C L, Xiao Y, Han Z, Dong C, Chen X, Cui J, Guo G and Sun F 2010 *J. Opt. Soc. Am. B* **27** 2495
[23] Yakubo K, Avishai Y and Cohen D 2003 *Phys. Rev. B* **67** 125319
[24] Lumerical Solutions http://www.lumerical.com/fdtd.php
[25] Palik E 1985 *Handbook of Optical Constants of Solids* (Academic)
[26] Yao Q F, Huang Y Z, Zou L X, Lv X M, Ling J D and Yang Y D 2013 *J. Lightwave Technol.* **31** 786
[27] Gartia M R, Lu M and Liu G L 2013 *Plasmonics* **8** 361
[28] Rottler A, Bröll M, Schwaiger S, Heitmann D and Mendach S 2011 *Opt. Lett.* **36** 1240